

Optimization of operating temperature in cryocooled HTS magnets for compactness and efficiency

Ho-Myung Chang ^{*,1}, Yeon Suk Choi, Steven W. Van Sciver

National High Magnetic Field Laboratory, Florida State University, 1800 E. Paul Dirac Dr., Tallahassee, FL 32310, USA

Received 22 July 2002; accepted 30 October 2002

Abstract

A new concept of thermal design to optimize the operating temperature of high temperature superconductor (HTS) magnets is presented, aiming simultaneously at small size and low energy consumption. The magnet systems considered here are refrigerated by a closed-cycle cryocooler, and liquid cryogenics may or may not be used as a cooling medium. For a specific magnet application, the size of required HTS windings could be smaller at a lower temperature, by taking advantage of a greater critical current density of HTS. As the temperature decreases, however, the power input to the cryocooler increases dramatically because of the heavy cooling load and the poor refrigeration performance. Through a rigorous modeling and analysis incorporating the effect of magnet size into the load calculation, it is demonstrated that there exists an optimum for the operating temperature to minimize the power required. The optimal temperature is strongly dependent upon the magnitude of AC loss in the magnets and the assistance of heat interception.

© 2003 Elsevier Science Ltd. All rights reserved.

Keywords: High T_c superconductors; Thermodynamics; Heat transfer; Power applications

1. Introduction

After the discovery of the high temperature superconductor (HTS), its successful fabrication into useful conductors has promised a great technical advance in numerous industrial areas, mainly because of the easy and economical cooling with liquid nitrogen at around 77 K. The commercial application of many HTS magnets, however, requires refrigeration at temperatures below 77 K, in order to take advantage of a greater critical current density of HTS and reduce considerably the size and weight of the system. Power devices such as HTS transformers, fault current limiters, motors, or generators [1–4] are some examples.

The cryogenic cooling at temperatures below 77 K can be conveniently achieved by employing a closed-cycle cryocooler. Two typical configurations of the cryocooled HTS magnet system are schematically shown in Fig. 1. The magnet may be immersed in a bath of

subcooled liquid nitrogen (or neon) continuously refrigerated by a cryocooler (Fig. 1a) or it may be directly conduction-cooled without any liquid (Fig. 1b). As the operating temperature of the magnet decreases, both the refrigeration load of the magnet and the required power per unit refrigeration at cryocooler increases dramatically. The excessive energy consumption or the degraded overall efficiency caused by a low temperature operation could seriously affect its competitiveness with the existing technology. Thus, the optimization of the cooling temperature aiming simultaneously at compactness and efficiency is one of the most critical issues in the commercialization of the HTS power devices.

In spite of its significance, only a few studies have been performed concerning the operating temperature of HTS magnets. Recently, Iwakuma et al. [2] and Funaki et al. [3] reported the feasibility of an HTS transformer in subcooled liquid nitrogen at round 65 K and the measurement of the AC loss for Bi-2223 windings. An economic analysis for the HTS power devices have been presented by Oomen et al. [4] as a preliminary investigation to exploit the capital investment and the operational cost for different sizes and operating temperatures. Still these reports have neglected the basic

* Corresponding author. Tel.: +1-850-644-0858; fax: +1-850-644-0867.

E-mail address: chang@magnet.fsu.edu (H.-M. Chang).

¹ On leave from Hong Ik University, Seoul, Korea.

Nomenclature

A	surface area or cross-sectional area (m^2)
d	thickness of HTS tape (m)
f	frequency of AC magnetic field (Hz)
g	gravitational acceleration (m/s^2)
I	current (A)
J_c	critical current density of HTS (A/cm^2)
k	thermal conductivity (W/(m K))
L	length of conductor or mechanical support (m)
L_0	Lorentz number ($(\text{W } \Omega)/\text{m}^2$)
M	mass of HTS magnet (kg)
Q	heat transfer rate (W)
S	safety factor of mechanical support
T	temperature (K)
V	volume of conductor (m^3)

W power input to cryocooler (W)

Greek symbols

ε	emissivity
σ	Stefan–Boltzmann constant ($\text{W}/(\text{m}^2 \text{K}^4)$), or yield strength (N/m^2)

Subscripts

ac	AC loss
H	warm (room-temperature) vessel
I	heat interception
k	conduction
L	cold HTS magnet
l	current lead
r	radiation
s	mechanical support

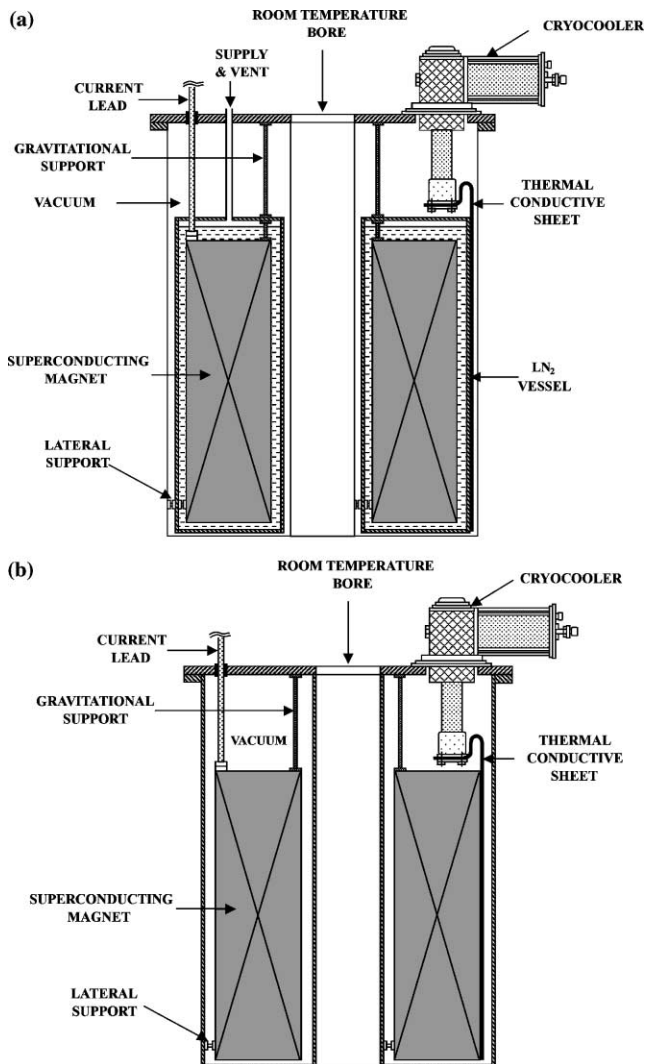


Fig. 1. Schematic configurations of typical HTS magnet systems refrigerated by a cryocooler: (a) liquid-cooling, (b) conduction-cooling.

thermal characteristics of the magnet and the cryogenic refrigeration.

An international collaborative research program directed to cryogenic systems for HTS power transformers is underway at the National High Magnetic Field Laboratory. The project aims at the design of compact and efficient cryogenic systems for both the Korean power industry and shipboard application for the US Navy. As a first step of these efforts, this paper presents a general and systematic approach to the optimization of HTS cooling temperature.

The concept of the proposed optimization is graphically shown in Fig. 2. Since this study is focused on the thermodynamic aspects of cryogenic refrigeration, it is assumed that the temperature of HTS magnet windings is spatially uniform, as being simply called the operating temperature. When a specific application goal (e.g. 1 MVA transformer) is given, the operating temperature of an HTS magnet can immediately affect the conductor size, because the critical current density of HTS varies with temperature. At the same time, the magnitude of cooling load caused by the several thermal or thermoelectric phenomena will be determined by both the operating temperature and the size of conductor. The refrigeration performance of a cryocooler being influenced also by the temperature will finally determine the power consumption in proportion to the magnitude of the cooling load. From the viewpoint of steady operation, the optimal cooling temperature should be found to minimize the power consumption, which is the main objective of the proposed investigation. Detailed issues on the winding design such as the effect of peak magnet field are beyond the scope of this thermodynamic optimization. A more practical and economic optimization might include the capital cost and the value of the compactness (indicated by dotted lines) in addition to

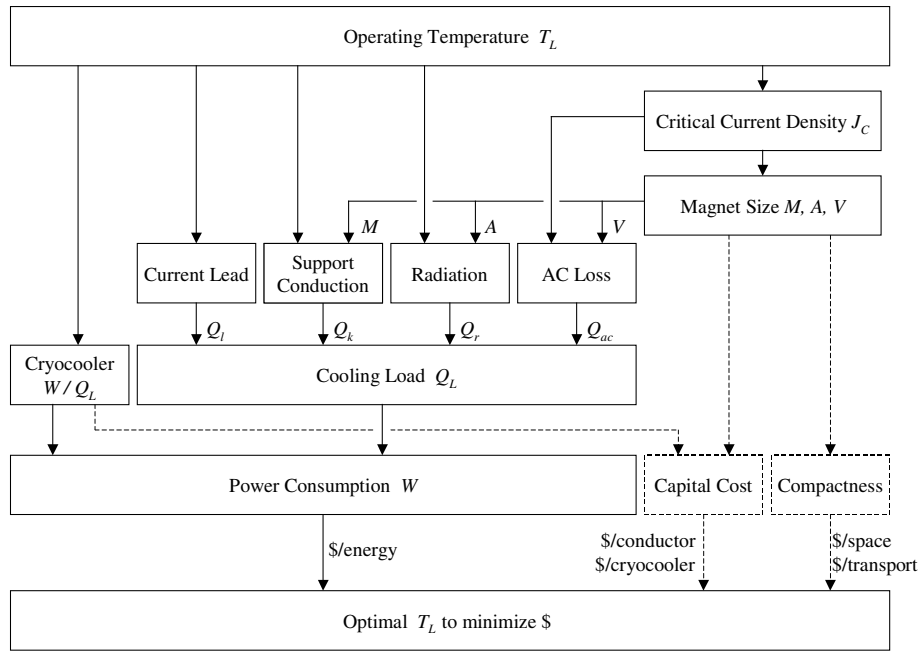


Fig. 2. Procedure to optimize the operating temperature for compactness and efficiency (solid lines indicate the present investigation).

the energy cost, but it will be also left for individual applications.

2. Cooling loads with magnet size

In the HTS magnet systems shown in Fig. 1, the cryogenic cooling requirements are continuously generated by four different physical mechanisms; thermal conduction through mechanical supports, thermal radiation, heat through current leads, and AC loss in HTS magnets. This section describes the models for the cooling load calculation that includes the quantitative effect of the operating temperature on the magnet size.

In practical design, it is not easy to determine the reduction in the size of an HTS magnet when the operating temperature is lowered to a particular level. It is generally true, however, that the amount of required HTS windings for a specified magnet goal is inversely proportional to the critical current density at the operating temperature, $J_c(T)$, if the operating current density is designed at a certain fraction (e.g. 50%) of J_c at the temperature and other variables are kept constant. In the following cooling load calculations, we may well take a simple model that the magnet size is inversely proportional to $J_c(T)$ of HTS.

2.1. Support conduction

The heat conduction through a mechanical support with constant cross-sectional area, A_s , is determined as

$$Q_k(T_L) = \frac{A_s(T_L)}{L_s} \int_{T_L}^{T_H} k_s(T) dT \quad (1)$$

where $k_s(T)$ is the temperature-dependent thermal conductivity and L_s is the length of the support. It should be noted in Eq. (1) that the magnet temperature, T_L , appears not only at the lower limit of integration but also in the cross-sectional area, because the supports of a lighter weight magnet would have a smaller cross-sectional area.

It follows that the cross-sectional area of the support can be proportional to the magnet mass, M , as

$$A_s(T_L) = S \frac{M(T_L)g}{\sigma_y} \quad (2)$$

if the mechanical safety factor, S , is given as a constant and the yield strength of the support material, σ_y , does not vary significantly over the temperature range. Since the mass of the HTS magnet is inversely proportional to $J_c(T_L)$ as assumed above, the temperature-dependence of the magnet mass can be expressed in terms of the reference values at liquid nitrogen temperature or 77 K.

$$M(T_L) = M(77 \text{ K}) \frac{J_c(77 \text{ K})}{J_c(T_L)} \quad (3)$$

A careful comparison is advised here between the mathematical involvement of the operating temperature in Eqs. (1)–(3) and the graphical illustration in Fig. 2. We expect clearly that as T_L decreases, the temperature span in the integration in Eq. (1) increases, but the required cross-sectional area decreases because $J_c(T)$ increases.

2.2. Radiation

The radiation heat transfer to a body at cryogenic temperature, T_L , from the enclosed surfaces at room temperature, T_H , can be approximately given by

$$Q_r(T_L) = \frac{\sigma(T_H^4 - T_L^4)}{\frac{1}{A_L(T_L)} \left(\frac{1-\varepsilon_L}{\varepsilon_L} + \frac{1}{F_{LH}} \right) + \frac{1-\varepsilon_H}{\varepsilon_H A_H}} \approx \frac{\sigma(T_H^4 - T_L^4)}{\frac{1}{\varepsilon_L A_L(T_L)} + \frac{1-\varepsilon_H}{\varepsilon_H A_H}} \quad (4)$$

since the view (or shape) factor from the cold to the warm surfaces, F_{LH} , is very close to unity [5]. A_L and A_H denote the external surface area of the cold body and the internal area of the room-temperature surface, respectively, and ε 's are the emissivity of the surfaces. In Eq. (4), the magnet temperature, T_L , is involved explicitly in the numerator and implicitly in A_L of the denominator. The temperature-dependence of the external surface area of the cold body, $A_L(T_L)$, will be even more complicated in practice, because it is associated with the detailed design of the HTS windings and the cooling options. It is assumed in this load calculation model that the volume of a cold body is proportional to the magnet size and the external surface area of the cold body has the two-third power of its volume from a dimensional consideration for similar shapes. Therefore, the temperature-dependence of A_L is expressed also in terms of the reference values at liquid nitrogen temperature.

$$A_L(T_L) = A_L(77 \text{ K}) \left[\frac{J_c(77 \text{ K})}{J_c(T_L)} \right]^{2/3} \quad (5)$$

The mathematical involvement of T_L in Eqs. (4) and (5) should be noted again with the graphical illustration in Fig. 2. As T_L decreases, both the numerator and the denominator of Eq. (4) increases, which means that the radiation per unit area increases but the external surface area of the magnet should decrease.

2.3. Current leads

Current leads are the major source of thermal load in all HTS magnets for power applications. The load is heat transfer to the cold end of the leads and may be different to a certain extent by the lead materials and the cooling methods. When the material is a metal obeying the Wiedemann–Franz Law and no boil-off gas is used for cooling as shown in Fig. 1, the size of the leads can be optimized such that the minimum cooling load per lead may be a function of the operating current, I , and the two end temperatures only [6,7].

$$Q_l(T_L) = I \sqrt{L_0(T_H^2 - T_L^2)} \quad (6)$$

where L_0 is the Lorentz number, $2.45 \times 10^{-8} \text{ (W}\Omega\text{)/K}^2$. The load due to current leads is directly dependent on the operating temperature of the HTS magnet, T_L , but

independent of the magnet size itself as indicated in Fig. 2.

2.4. AC loss

Alternating magnetic fields and transport currents cause dissipation and this energy dissipation is called AC loss. The critical-state model [4] predicts that for a rectangular tape with field parallel to the flat surface the AC loss per unit volume of conductor depends on the applied field (B), the frequency of magnetic field change (f), and the thickness of the HTS tape (d). Since the AC loss per unit volume is proportional to the critical current density in the model when the magnetic field is greater than the penetration field, the amount of total AC loss is expected to be principally temperature-independent. Therefore, the AC loss can be expressed as

$$Q_{ac}(T_L) = Bfd \frac{I}{I_c} V(T_L) J_c(T_L) = BfdLI \quad (7)$$

where L is the length of conductor. Eq. (7) is valid when the HTS tape is oriented parallel to the magnetic field or the self-field is dominant in the magnet. Fig. 2 also indicates that the AC loss is determined in general by the critical current density and the conductor volume, being influenced by the operating temperature. From the thermodynamic point of view, the AC loss should be distinguished from other three loads because it is a dissipation at T_L and has nothing to do with the temperature difference between T_H and T_L .

3. Power consumption at cryocooler

All the cooling loads described above should be removed by a cryocooler in order to maintain a steady state at the operating temperature. Fig. 3 shows schematically the energy balance at the HTS magnet for single-stage or two-stage cooling. The power consumed at cryocooler is the object function to be minimized in this optimization. The power requirement is now estimated from the cooling loads, Q_L , and the cryocooler performance, which should be characterized by the power input per unit refrigeration, W/Q_L , as indicated in Fig. 2.

3.1. Single-stage cooling

In general, the power per unit refrigeration of a single-stage cryocooler that absorbs heat at T_L and rejects heat at room temperature, T_H , can be expressed as

$$\frac{W}{Q_L} = \frac{1}{\text{FOM}_L} \left(\frac{T_H}{T_L} - 1 \right) \quad (8)$$

where FOM_L is the figure of merit [8] or Carnot efficiency of the cryocooler. The term, $T_H/T_L - 1$, in Eq. (8)

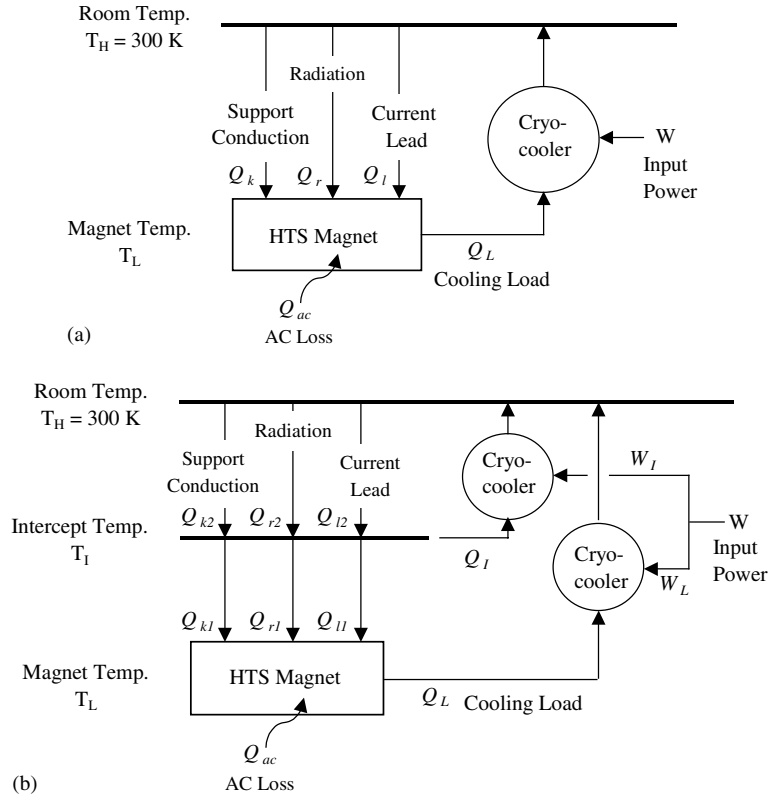


Fig. 3. Energy balance at HTS magnet system: (a) single-stage cooling, (b) two-stage cooling.

is the minimum power per unit refrigeration that can be obtained when $FOM_L = 1$ or every process is reversible. The power required for single-stage cooling can be generally expressed as a complicated function of T_L .

$$W(T_L) = \frac{1}{FOM_L} \left(\frac{T_H}{T_L} - 1 \right) [Q_k(T_L) + Q_r(T_L) + Q_l(T_L) + Q_{ac}(T_L)] \quad (9)$$

where Q 's are determined by Eqs. (1), (4), (6) and (7).

3.2. Two-stage cooling

An effective method to save the input power for the refrigeration is the heat intercept. In order to reduce the heat leak to the magnet at T_L , heat can be partly removed at an intermediate temperature, T_I , from the mechanical supports and the current leads, and a radiation shield cooled at the same temperature, T_I , can be placed in vacuum. In the energy balance shown in Fig. 3(b), the subscripts 1 and 2 of Q 's denote the heat leaks from T_I to T_L and from T_H to T_I , respectively. As a result of the heat intercept, two cooling loads are assigned at two different temperatures; Q_I at T_I and Q_L at T_L . The two-stage refrigeration may be performed with two different units of single-stage cryocooler or a two-stage cryocooler. When a two-stage cooler is used, the esti-

mates of the actual power input could be rather complicated, because the refrigeration at the two stages are coupled each other. For the purpose of thermodynamic design, we assume here that the total power is simply the sum of power for the heat intercept, W_I , and the power for the refrigeration of magnet, W_L .

$$W(T_I, T_L) = W_L(T_I, T_L) + W_I(T_I, T_L) \quad (10)$$

The cooling load at the magnet temperature, T_L , due to support conduction, radiation, and current leads, can be simply determined with replacing T_H by T_I in Eqs. (1), (4) and (6), respectively. The power required for the load at T_L is expressed as

$$W_L(T_I, T_L) = \frac{1}{FOM_L} \left(\frac{T_H}{T_L} - 1 \right) [Q_{k1}(T_I, T_L) + Q_{r1}(T_I, T_L) + Q_{l1}(T_I, T_L) + Q_{ac}(T_L)] \quad (11)$$

The first three cooling loads in Eq. (11) are less than those in single-stage cooling, since T_I is smaller than T_H , but the AC loss is the same, since it is independent of the heat intercept. Similarly, the heat leaks from the room-temperature to the intercept stage due to support conduction, radiation, and current leads, are determined by replacing T_H by T_I in Eqs. (1), (4) and (6), respectively. The heat intercept at T_I should be the difference between Q_2 's and Q_1 's.

$$W_1(T_1, T_L) = \frac{1}{\text{FOM}_1} \left(\frac{T_H}{T_1} - 1 \right) \{ [Q_{k2}(T_1) - Q_{k1}(T_1, T_L)] + [Q_{r2}(T_1) - Q_{r1}(T_1, T_L)] + Q_{l2}(T_1) \} \quad (12)$$

The last term in Eq. (12) does not include the heat through the leads from T_1 to T_L , because the axial temperature gradient at the warm end should be zero for all optimized metallic leads [6,7].

4. Results and discussion

The objective of this optimization is to determine the operating temperature of an HTS magnet that requires the minimum power consumption for cryogenic refrigeration. While the modeling and analysis procedure presented in previous sections may be applicable to any cryocooled HTS magnets, a specific situation is considered here for the purpose of quantitative discussion. Table 1 is an example of selected specifications for a 1 MVA single-phase HTS transformer magnet [2]. The temperature-dependent variables given in Table 1 are the reference values at liquid nitrogen temperature, 77 K.

The most common HTS conductor in power applications is Bi-2223/Ag tape. The critical current density, $J_c(T)$, of Bi-2223 is represented within acceptable accuracy as a function of temperature [1]:

$$J_c(T_L) = J_{c0} \left(1 - \frac{T_L}{104} \right)^{1.4} \quad (13)$$

where J_{c0} is the critical current density at 0 K. The ratio of $J_c(T)$ to its value at 77 K is expressed as

$$\frac{J_c(T_L)}{J_c(77 \text{ K})} = \frac{\left(1 - \frac{T_L}{104} \right)^{1.4}}{\left(1 - \frac{77}{104} \right)^{1.4}} = 6.61 \left(1 - \frac{T_L}{104} \right)^{1.4} \quad (14)$$

The functional relation of Eq. (13) is now used to calculate the cooling load including the magnet size in Eqs. (3) and (5). Wolsky [1] predicts the superconducting tape

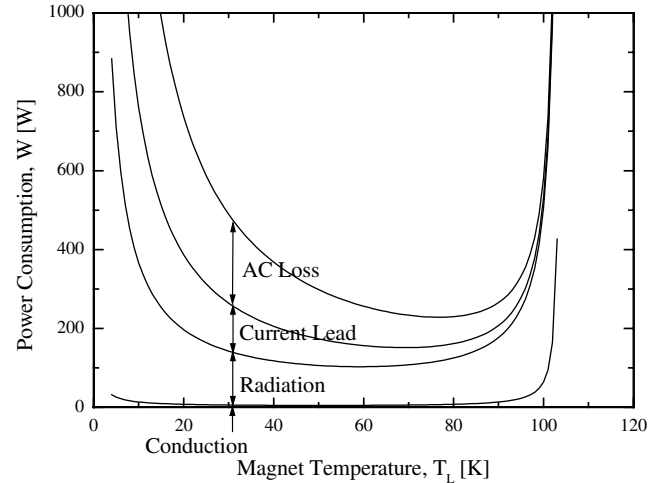


Fig. 4. Sum of power consumptions contributed by each cooling load as a function of operating temperature for single-stage cooling.

whose AC loss is 0.25 W/(kA m) will be developed. We take the AC loss in this analysis simply as

$$Q_{ac}(T_L) = (0.25 \times 10^{-3})LI \quad (15)$$

This value is simply an optimistic expectation for typical power applications, but could be approximately true from Eq. (7) when B (parallel field) = 0.05 T, f = 50 Hz, d (effective thickness) = 0.1 mm, as in typical case of HTS transformer windings.

Fig. 4 shows the power consumption calculated with Eq. (9) as a function of operating temperature for single-stage cooling. The sum of the power consumption is subdivided into the four portions, indicating the contributions of individual cooling load. Over a wide temperature range, the AC loss and the radiation are dominant in the contributions. In the calculation, the FOM of cryocooler has been 1 or the so-called Carnot limit has been assumed, to demonstrate the thermodynamic nature of the optimization. The effect of actual cryocooler performance will be briefly discussed later.

Table 1
Specifications of HTS magnet system at 77 K for sample calculation

HTS windings (Bi-2223/Ag)	Current (primary/secondary)	I	45.5 A/145 A
	Mass at 77 K	M (77 K)	282 kg
	External surface area at 77 K	A_L (77 K)	4.2 m ²
	Emissivity (polished Ag)	ϵ_L	0.02
Mechanical support (Stainless steel)	Length	L_s	0.3 m
	Yield strength	σ_y	207×10^6 Pa
	Safety factor	S	20
Radiation shield ^a (Aluminum)	Surface area at 77 K	A_R (77 K)	5.5 m ²
	Emissivity	ϵ_R	0.1
Cryostat (GFRP)	Internal surface area	A_H	6.9 m ²
	Emissivity	ϵ_H	0.88
	Room temperature	T_H	300 K

^a Only for two-stage cooling.

As T_L decreases to below 30 K, the power consumption increases dramatically, since both the cooling load and the power per unit refrigeration increase. On the other hand, as T_L increases toward 104 K (the critical temperature of HTS), $J_c(T)$ of the HTS conductor shrinks and a greater size of magnet should be needed for the specified application goal. A greater cooling load due to conduction and radiation would result in the growth of total power at higher temperatures near 104 K. There exists a unique optimum for the operating temperature to minimize the power consumption. Since the optimization of the operating temperature has quite different features depending upon the existence of the AC loss, DC and AC magnets will be discussed separately.

In case of the heat intercept or the two-stage cooling, the total input power is a function of not only the magnet temperature, T_L , but also the intercept temperature, T_I , as indicated in Eq. (9). Fig. 5 shows the power calculated with Eq. (10) as a function of T_I for the DC magnet, when T_L is fixed at 20 K. There exists an obvious minimum power of 135 W around at $T_I = 170$ K. It should be observed carefully that W_I vanishes as T_I approaches asymptotically to T_H , and W_L vanishes as T_I approaches asymptotically to T_L . Since the two-stage-cooling turns out to be a single-stage in both extreme cases, the total power must have a minimum between the two end temperatures. Once the intercept temperature is designed at the optimum, the total power for two-stage cooling can be considered as a function of T_L only as discussed below.

4.1. DC magnets

In DC magnets where the AC loss does not exist in the cooling load, the required power has a local minimum of

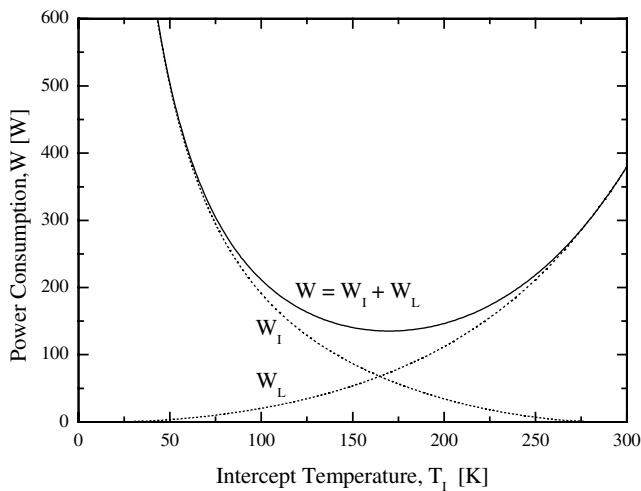


Fig. 5. Power consumption as a function of intercept temperature when $T_L = 20$ K for two-stage cooling.

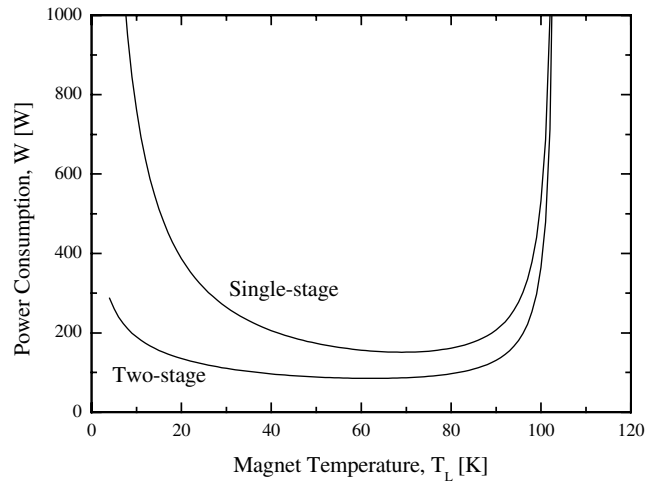


Fig. 6. Power consumption for DC magnet (intercept temperature optimized for two-stage cooling).

151 W approximately at $T_L = 69$ K as indicated by single-stage in Fig. 6. One of the most significant facts in a DC magnet is that the curve for the power consumption is very flat over a wide temperature range between 50 and 80 K around the optimum. This implies that an operating temperature well below the optimum would result in only a small increase in the cost of steady operation but a great reduction in size and cost of magnet. In other words, the optimum of T_L will shift further down if the capital investment and the economic merits of compactness are involved as indicated in Fig. 2.

In practice, the FOM of a cryocooler varies with T_L to a certain extent, but depends more significantly upon the thermodynamic cycle and the refrigeration capacity. Most of the contemporary cryocoolers have the values between 0.1 and 0.3 in the interested temperature range, thus the actual power for the cryocooler is expected to vary from 500 W up to 1.5 kW at the optimal condition.

The two-stage cooling with the optimized heat intercept is also compared in Fig. 6 with the single-stage cooling. The optimum of T_L with two-stage cooling is around 62 K (nearly the freezing temperature of nitrogen) and the minimum power can be decreased to 85 W. An obvious advantage of the two-stage cooling is, however, justified only at temperatures lower than 30 K, since the power saving is substantial.

4.2. AC magnets

Most of the magnets in power application are AC magnets and have significant amount of AC loss. Fig. 7 shows the required power for the cooling load including the AC loss in the same situation as above. Because of the additional load, the minimum required power is raised to 229 W and the corresponding optimal T_L is as high as 77 K (nearly the normal boiling temperature of

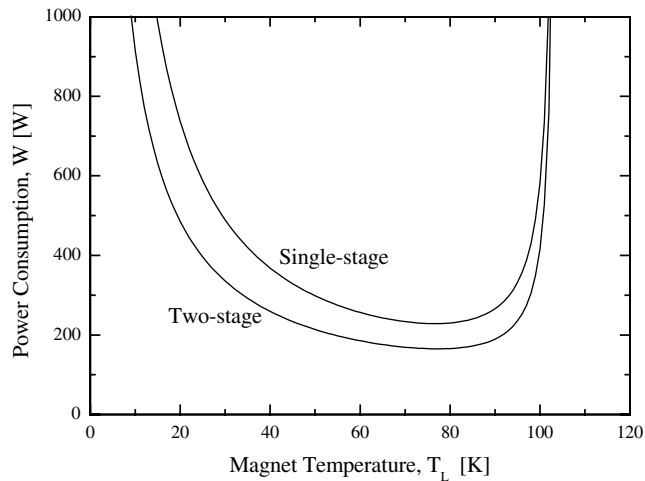


Fig. 7. Power consumption for AC magnet (intercept temperature optimized for two-stage cooling).

nitrogen). The reason for the higher value of optimal T_L is that the refrigeration of the AC loss has a greater impact at lower temperatures. In the optimum temperature, the actual power consumption would be 760 W to 2.3 kW with commercially available cryocoolers, FOM of which has a value between 0.1 and 0.3.

It is still true for AC magnets that the optimal operating temperature in practice becomes lower than the calculated value, if the capital investments and the economic merits of compactness are considered in addition to the operational costs at steady state. However, the curve shape around the local minimum for AC magnets is not so flat as that of DC magnets, which means that the operating temperature of AC magnets should not be so low as that of DC magnets with the same economic factors.

Another remarkable feature in Fig. 7 is that the power saving by two-stage cooling is only a small amount even for very low temperature operation of HTS magnets. It should be emphasized again that the AC loss is the dissipation at cryogenic temperatures which must accept a heavy penalty of thermodynamic irreversibility, while the other cooling load is a heat leak from the room temperature that can be intercepted before reaching the cryogenic temperatures. Therefore, no heat intercept or the two-stage cooling is recommended even when the HTS magnet is operated at temperatures below 30 K, if the AC loss is dominant in the cooling load.

5. Conclusions

A comprehensive thermal design is performed in pursuit of compactness and high efficiency in the cooling of HTS magnets. The optimum operating temperature is

sought to minimize the power consumption in steady operation, by taking into account the critical properties of HTS affecting the magnet size, the cooling load estimate, and the basic refrigeration characteristics of cryocooler. For a specified application goal, the HTS magnet could be best refrigerated at temperatures between 62 and 77 K, depending upon the magnitude of AC loss and the assistance of heat intercept. The presented optimum in the operating temperature for AC magnets may vary to a large extent with the amount of AC loss, as it is crucially affected by the magnetic field. It is also concluded that the operating temperature could be determined at considerably lower level, if the capital investments and the costs associated with installation space or transportation of the compact HTS magnets are added to the operational cost. The presented optimization will be immediately applied to the basic design of an efficient cooling system for HTS power devices.

Acknowledgements

This research is supported by a joint grant from the CAST (Center for Applied Superconductivity Technology) under the 21st Century Frontier R&D Program funded by the Ministry of Science and Technology, Korea and the CAPS (Center for Advanced Power Systems) with the NHMFL (National High Magnetic Field Laboratory).

References

- [1] Wolsky AM. Cooling for future power sector equipment incorporating ceramic superconductors. The IEA Implementing Agreement for a Co-Operative Programme for Assessing the Impacts of High-Temperature Superconductivity on the Electric Power Sector. Argonne National Laboratory Report. April 2002. Available from: <http://www.iea.org/tech/scond/scond.htm>.
- [2] Iwakuma M, Funaki K, Kajikawa K, Tanaka H, Bohno T, Tomioka A, et al. AC loss properties of a 1 MVA single-phase HTS power transformer. *IEEE Trans Appl Supercond* 2001;11:1482–5.
- [3] Funaki K, Iwakuma M, Kajikawa K, Hara M, Suehiro J, Ito T, et al. Development of a 22 kV/6.9 kV single-phase model for a 3 MVA HTS power transformer. *IEEE Trans Appl Supercond* 2001;11:1578–81.
- [4] Oomen MP, Haken B, Leghissa M, Rieger J. Optimum working temperature of power devices based on Bi-2223 superconductors. *Supercond Sci Technol* 2000;13:L19–24.
- [5] Rohsenow WM, Choi HY. Heat, mass, and momentum transfer. New Jersey: Prentice-Hall; 1961. p. 332–51.
- [6] Chang H-M, Van Sciver SW. Thermodynamic optimization of conduction-cooled HTS current leads. *Cryogenics* 1998;38:729–36.
- [7] Wilson MN. Superconducting magnets. Oxford: Oxford University Press; 1983. p. 256–60.
- [8] Barron RF. Cryogenic systems. 2nd ed Oxford: Oxford University Press; 1985. p. 237–40.